Effects of Soret, Dufour, Hall currents and thermal radiation on a steady mixed convective heat and mass transfer over a stretching sheet in a rotating fluid

G. Sarojamma, S. Mahaboobjan, K. Sreelakshmi

Abstract— The non – linear boundary layer flow of a viscous incompressible electrically conducting fluid over a linearly stretching sheet in a rotating fluid in the presence of Hall currents, thermal radiation, heat source/ sink with Soret and Dufour effects. The partial differential equations governing the flow are numerically solved using fourth order Runge – Kutta method together with shooting technique. The Coriolis force reduces both the primary and secondary velocities while it enhances the temperature distribution. The magnetic field reduces (increases) the primary velocity (secondary velocity) and enhances the temperature where as the Hall parameter produces an opposite effect. The heat source, thermal radiation and Dufour effect favor heat transfer. In the range of Df = 1 - 3, the skin friction coefficient increases with increasing Soret number while an opposite trend when Df = 4 is noticed. The Dufour number decreases the Sherwood number in the range 0.1 – 0.85 of Soret number while a reverse trend is observed for Sr > 0.85.

Index Terms— MHD, Hall current, Rotation effect, Stretching sheet.

1 Introduction:

The study of flows due to a stretching surface in a viscous fluid is of significant importance as this type of motion occurs in the extrusion of polymer fibers and films. Many metallurgical processes which involve drawing annealing and tinning of wires require cooling of the sheets or fibers by stretching them through a rotating fluid. The quality of the end product depends on the rate of cooling. Sakiadis [1] was the first researcher to study the classical problem of steady flow on a stretching surface extended from a slit.

- *Author name is Prof. G. Sarojamma working as Professor of Applied Mathematics, Sri Padmavati Women's University, Andhra Pradesh, India. E-mail: gsarojamma@gmail.com*
- *Co-Authors S. Mahaboobjan, K. Sreelakshmi are working as a Research Sholars in Department of Applied Mathematics,Sri Padm avati Women's University, Andra Praesh,India,E.mail:smahaboobj an@rediffmail.com,katasreelakshmi@gmail.com*

Crane [2] investigated the steady flow on a stretching surface in a quiescent fluid and obtained an analytical solution. Subsequently he [3] investigated the corresponding heat transfer problem. Following these studies several authors studied various aspects of this problem. Wang [4] made an analysis of the steady flow on a stretching sheet in a rotating fluid. Takhar et al [5] investigated the boundary layer flow of a viscous incompressible conducting fluid over a moving surface in a rotating fluid with Hall currents and free stream velocity. Anika et al [6] studied the effects of Hall currents on the unsteady flow and heat transfer of a viscous incompressible fluid past a vertical porous plate embedded in a rotating fluid. They observed that the rotation parameter decreases primary and secondary velocities and increases temperature.

In the present investigation an attempt is made to study the laminar mixed convection heat and mass transfer of a viscous incompressible, electrically conducting fluid over a vertical stretching surface embedded in a rotating fluid. The effects of Soret and Dufour thermal radiation and heat generation/absorption with Hall currents are considered.

2 Formulation:

The physical configu ration and co-ordinate system are presented in Fig.1. We consider the steady laminar boundary layer flow and mixed convection heat and mass transfer of an incompressible, viscous electrically c onducting fluid over a vertical stretching surface embedded in a fluid rotating with an angular velocity Ω about y – axis. The stretching surface has a linear velocity. The magnetic field of strength B_0 is applied normal to the surface. All the physical properties of the fluid are assumed to be constant. The effect of Coriolis force and Hall current give rise to a force in the z – direction which induces a cross flow in the z- direction. Consequently the flow becomes three dimensional. Using the Rosseland approximation the radiative heat flux is incorporated in the energy equation. The stretching surface has a fixed temperature T_w and the free stream temperature is T_∞ with $T_w > T_\infty$. The surface is also assumed that it has a uniform concentration C_w and the free stream concentration is C_∞ with $C_w > C_\infty$. The Soret and Dufour effects and chemical reaction are considered.

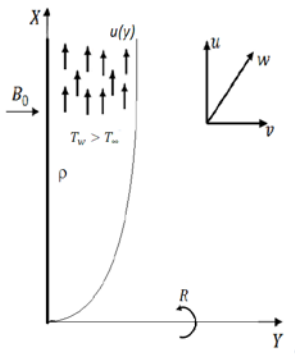

Fig. 1 Physical model and coordinate system

The generalized Ohm's law can be written as

$$\bar{J} = \sigma\,(\bar{E} + \bar{V} \times \bar{B}) - \frac{\sigma}{e\eta}(\bar{J} \times \bar{B} - \nabla\rho_e)$$

Here $\bar{V}$ is the velocity vector, $\bar{B}$ is the magnetic induction vector, $\bar{E}$ is the electric field vector, σ is the electrical conductivity, ρ_e is the electronic pressure. Using the Boussinesq's approximation the boundary layer equations governing the flow in a rotating frame of reference can be written as

Equation of continuity:

$$\frac{\partial u}{\partial x} + \frac{\partial v}{\partial y} = 0 \qquad (1)$$

Momentum equations:

$$u\frac{\partial u}{\partial x} + v\frac{\partial u}{\partial y} = \nu\frac{\partial^2 u}{\partial y^2} + g\beta(T - T_\infty) + g\beta^*(C - C_\infty) - \frac{\sigma B_0^2}{\rho(1+m^2)}(u + mw) + 2\Omega w \qquad (2)$$

$$u\frac{\partial w}{\partial x} + v\frac{\partial w}{\partial y} = \nu\frac{\partial^2 w}{\partial y^2} + \frac{\sigma B_0^2}{\rho(1+m^2)}(mu - w) - 2\Omega u \qquad (3)$$

Energy equation:

$$u\frac{\partial T}{\partial x} + v\frac{\partial T}{\partial y} = \frac{1}{\rho c_p}\left[K\frac{\partial^2 T}{\partial y^2} - \frac{\partial q_r}{\partial y} + Q_0(T - T_\infty)\right] + \frac{D_m K_T}{C_s C_p}\frac{\partial^2 C}{\partial y^2} \qquad (4)$$

Concentration equation:

$$u\frac{\partial C}{\partial x} + v\frac{\partial C}{\partial y} = D\frac{\partial^2 C}{\partial y^2} - k(C - C_\infty) + \frac{D_m K_T}{T_m}\frac{\partial^2 T}{\partial y^2} \qquad (5)$$

Subject to the boundary conditions

$$u = bx,\ v = 0,\ w = 0,\ T = T_w(x, t),\ C = C_w(x, t) \text{ at } y = 0,$$

$$u \to 0,\ v \to 0,\ T \to T_\infty,\ C \to C_\infty \text{ as } y \to \infty \qquad (6)$$

where u, v and w are the fluid velocity components along x, y and z axes, respectively, ν is the kinematic viscosity, g is the acceleration due to gravity, B_0 is the strength of the magnetic field, β is the volumetric coefficient of thermal expansion, β^* is the coefficient of expansion with concentration, ρ is the density of the fluid, T is the fluid temperature, C is the fluid concentration, K is the thermal conductivity of the medium, c_s concentration susceptibility, q_r is the radiation heat flux, C_p is the specific heat at constant pressure, Q_0 is the uniform volumetric heat generation and absorption, D is the mass diffusivity, k is the chemical reaction parameter D_m is the coefficient of mass diffusivity, T_m is the mean fluid temperature and K_T is the thermal-diffusion ratio.

The radiation heat flux using Rosseland approximation can be written as

$$q_r = -\frac{4\sigma_s}{3k^*}\frac{\partial T^4}{\partial y} \qquad (7)$$

where σ_s is the Stefen-Boltzman constant and k^* is the absorption coefficient. T^4 may be linearly expanded in a Taylor's series about T_∞ to get

$$T^4 = 4T_\infty^3 T - 3T_\infty^4 \qquad (8)$$

To examine the flow regime adjacent to the sheet, the following transformations are invoked

$$u = bxf'(\eta)\,; v = \sqrt{b\nu}f(\eta)\;;\; w = bxh(\eta)\,; \eta = \sqrt{\frac{b}{\nu}}y \quad (9)$$

$$T = T_\infty + (T_w - T_\infty)\,\theta(\eta), \quad (10)$$

$$C = C_\infty + (C_w - C_\infty)\,\phi(\eta), \quad (11)$$

From the above transformations, the equations (2) – (5) reduce to the non – dimensional, nonlinear and coupled ordinary differential equations

$$f''' + ff'' + G_r\theta + G_c\phi - \frac{M}{1+m^2}(f' + mh) + 2\lambda h = 0 \quad (12)$$

$$h'' + fh' + \frac{2M}{1+m^2}(mf' - h) - 2\lambda f' = 0 \quad (13)$$

$$\theta'' + \frac{Pr}{1+Nr}(f\theta' - \alpha\theta + Df\phi'') = 0 \quad (14)$$

$$\phi'' + Sc(f\phi' - \gamma\phi + Sr\theta'') = 0 \quad (15)$$

The pertinent boundary conditions are

$$\eta = 0:\; f = 0, f' = 1, h = 0, \theta = 1, \phi = 1,$$

$$\eta \to \infty:\; f' \to 0, h \to 0, \theta \to 0, \phi \to 0,$$

where the primes denote the differentiation with respect to η, $\lambda = \Omega/b$ is the rotation parameter which represents Coriolis force, $M = \sigma B_0^2/\rho b$ is the magnetic parameter, $G_r = \frac{g\beta_T(T_w - T_\infty)}{b^2 x}$ is the local thermal Grashof number $G_c = \frac{g\beta_c(C_w - C_\infty)}{b^2 x}$ is the local solutal Grashof number, $\gamma = k/b$ the non – dimensional chemical reaction parameter, $Pr = \rho c_p \nu/k$ is the Prandtl number , $N_R = 16\sigma_s T_\infty^3/3Kk^*$ is the thermal radiation parameter, $\alpha = Q_0/\rho b\, c_p$ is temperature dependent heat source/sink parameter, $Sc = \nu/D_m$ is the Schmidt number $Df = D_m K_T(C_w - C_\infty)/C_s C_p \nu$ is the Dufour number, and $Sr = D_m K_T(T_w - T_\infty)/\nu\, T_m(C_w - C_\infty)$ is the Soret number.

The physical quantities of interest in this problem are the skin friction coefficient C_f, local Nusselt number Nu_x and local Sherwood number Sh_x which are defined as

$$C_f = \frac{2\mu(\partial u/\partial y)_{y=0}}{\sqrt{Re_x}},\ \mathrm{Nu}_x = -\frac{x(\partial T/\partial y)_{y=0}}{T_w - T_\infty},$$

$$Sh_x = -\frac{x(\partial C/\partial y)_{y=0}}{C_w - C_\infty}$$

$$\frac{1}{2}C_f\sqrt{Re_x} = f''(0),\ \mathrm{Nu}_x/\sqrt{Re_x} = -\theta'(0),$$

$$Sh_x/\sqrt{Re_x} = -\phi'(0),$$

where $\mu = k/\rho c_p$ is the dynamic viscosity of the fluid and $Re_x = x\,U_w/\nu$ is Reynolds number.

3 Results and Discussion:

In this investigation the effect of rotation on the flow heat and mass transfer of an incompressible fluid past a stretching sheet in the presence of Hall currents, Soret and Dufour effects is studied. The governing non-linear coupled ordinary differential equations are solved numerically satisfying the boundary conditions for parametric values of magnetic field parameter M, Hall parameter m, thermal buoyancy number Gr, solutal buoyancy number Gc, rotation parameter λ ,thermal radiation parameter Nr, Prandtl number Pr, temperature dependent heat source α, Dufour number Df, Soret number Sr, Schmidt number Sc and chemical reaction parameter γ using the fourth order Runge – Kutta method together with shooting technique. The effect of various parameters on the flow variables is examined and discussed. In order to ensure the accuracy of the numerical method we have compared the present results when M = m = Du = Sr = 0 with those of Wang [4] and Nazar et al [7] as shown in Table. 1 for different values of the skin friction coefficient in the x and y directions $f''(0)$ and $h'(0)$ respectively and it is observed that they are in good agreement.

The influence of magnetic parameter M on the velocities, temperature and mass concentration is depicted in Figs. 2-5 with Gr=0.5; m=0.1; $\lambda = 0.5$; Gc=0.5; Pr=0.72; α=1.0; Df=0.5; Sr=0.5; γ=1; Nr=1.0; Sc=0.5. The primary velocity is reduced for increasing values of the magnetic field parameter throughout the boundary layer and hence the boundary layers become thinner. This is in view of the retarding nature of the Lorentz force. However, it is noticed that the secondary velocity is totally negative and shows an enhancing trend with increasing M. The temperature and concentration distributions are observed to be increasing with M.

The influence of Hall parameter m on the flow variables is shown in Figs. 6-9. The behavior of primary and secondary velocities for a variation in the Hall parameter is exactly opposite to that of the magnetic field. However, the secondary velocity is significantly influenced by the Hall parameter in the vicinity of the surface. Similarly the temperature and concentration are decreased with m.

The variation of the rotation parameter λ on the flow variables is illustrated in Figs. 10-13. The primary velocity is reduced with increasing rotation parameter. The reduction is more for higher values of $\lambda = 0.75, 1$. For $\lambda = 0.25$ the variation is very small. The secondary velocity is significantly influenced by the rotation parameter when $\lambda > 0.75$. There is a reduction in the velocity, when $\lambda = 1$ the reduction in the velocity is more than twice to that corresponding to the case when $\lambda = 0.5$. The temperature and concentration distributions are observed to be increasing with increasing λ. However, the increase is steady.

The effect of thermal buoyancy parameter Gr is presented in Figs. 14-17. The primary velocity is increased for increasing Gr while the secondary velocity is decreased. Thus the thickness of the boundary layers increases in the x – direction while it reduces in the y – direction. It is observed that the thermal and the solutal boundary layers become thinner for increasing Gr. Figs.18-21 indicate that the effect of solutal buoyancy parameter on the above variables is found to be similar to that of Gr.

The influence of Prandtl number on the flow variables is presented in Figs. 22-25. The primary velocity is reduced due to the reduction in the thickness of the boundary layer. The secondary velocity does not show much variation near the boundary. But it starts increasing away from the boundary. The thermal boundary layer thickness decreases with increasing values of the Prandtl number with a fall in the temperature. This may be attributed to the fact that increase in the Prandtl number amounts to decrease in the thermal conductivity. The concentration is observed to increase very nominally with increasing Pr.

The effect of the radiation parameter Nr is illustrated in Figs. 26-29 the primary velocity is found to increase with increasing Nr away from the boundary. However, the secondary velocity follows an opposite trend. The temperature increases significantly throughout the thermal boundary layer, which can be attributed to the fact that increasing values of Nr correspond to enhancement of thermal radiation in the thermal boundary layer resulting in the rise of the temperature in the thermal boundary layer. The concentration decreases with increasing Nr and this reduction is negligible.

Figs. 30-33 depict the influence of temperatu re dependent heat source on velocity, temperature and concentration. It is evident that increasing values of α increase both components of velocity, temperature of the fluid and concentration. This may be attributed to the fact that the presence of a heat source ($\alpha > 0$) would generate energy resulting a rise in temperature. Further, the temperature on the stretching surface is higher than the temperature in the fluid hence the heat transfer takes place from the surface to the fluid. This in turn would enhance the flow field owing to the buoyancy effect. On the contrary, when $\alpha < 0$ (heat sink) an opposite effect, viz., cooling of the fluid occurs. Consequently the thickness of the thermal boundary layer is reduced (Figs 34-37).

Figs. 38-41 show the effect of Dufour number on the flow variables. Both primary and secondary velocities increase with increasing Dufour number. The temperature enhances throughout the region. When Df = 7 there is an over shoot of the temperature. This may be attributed to the fact that energy is released as a result of the large concentration gradients. Thus the Dufour parameter increases the thickness of the thermal boundary layer. With increase in Df, the solutal boundary layer becomes thinner and thinner with a fall in the concentration.

In figs. 42-45 the variation of Soret number is presented. It is observed that the primary velocity enhances while the secondary velocity component decreases. The Soret number decreases the thickness of the thermal boundary layer with a fall in the temperature. Contrary to the Dufour effect on concentration, the concentration increase with increasing Soret number. For higher values of $Sr \geq 5$ the concentration exceeds the actual prescribed value on the surface. The solutal boundary layers also become thicker for increasing values Sr.

The effect of chemical reaction parameter γ on the velocities, temperature and concentration is depicted in figs. 46-49. The primary velocity decreases and the secondary velocity increases with increasing chemical reaction parameter. The thermal

boundary layer becomes thinner for increasing γ. The species concentration decreases as the chemical reaction parameter increases. Also it gradually decreases from its prescribed value on the surface to its lower value eventually satisfying the boundary condition as $\eta \rightarrow \infty$.

Figs. 50-53 present the influence of Schmidt number Sc on the flow variables. The velocity component in the x – direction reduces while the y component increases for increasing values of Sc. The thickness of thermal boundary layer with a enhancement in the temperature. The concentration is significantly reduced for increasing Sc as increasing values of Sc amounts to increase in molecular diffusivity.

Table 2 presents the skin friction coefficient in the x and y – directions, local Nusselt number and local Sherwood number. Positive values of skin friction coefficient indicate that the fluid exerts a drag force on the sheet while negative values correspond to the reverse effect. The skin friction coefficient in the x – direction decreases with magnetic field parameter, Pr, γ , Sc, $\alpha < 0$ while it increases with Hall parameter, Gr, Gc, $\alpha > 0$, Nr, Df and Sr whereas its corresponding component in the y – direction shows an opposite trend. The rotation parameter decreases skin friction coefficient in both the directions. It is noticed that the magnetic paramet er, Hall parameter, rotationn parameter, heat source parameter $\alpha > 0$, thermal radiation parameter, Dufour parameter, chemical reaction parameter and Schmidt number favor heat transfer. The local Nusselt number increases with Gr, Gc, Pr, $\alpha < 0$, the local Sherwood number decreases with M, λ, Pr, $\alpha > 0$, Sr. while the parameter m, Gr, Gc, $\alpha < 0$, Df, γ and Sc enhance the Sherwood number.

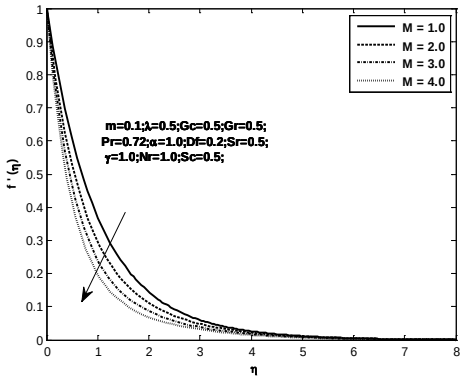

Fig. 2. Variation of f '(η) with η for different values of M

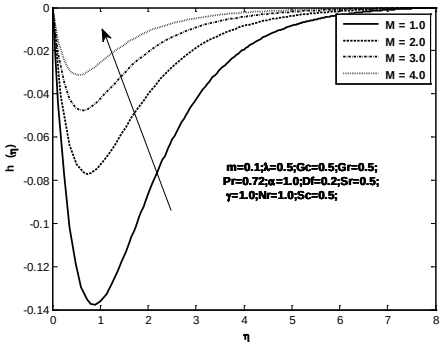

Fig. 3. Variation of h(η) with η for different values of M

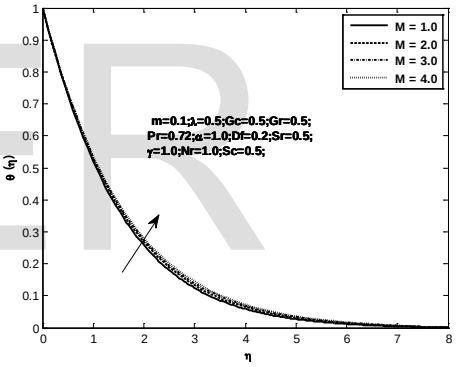

Fig. 4. Variation of θ(η) with η for different values of M

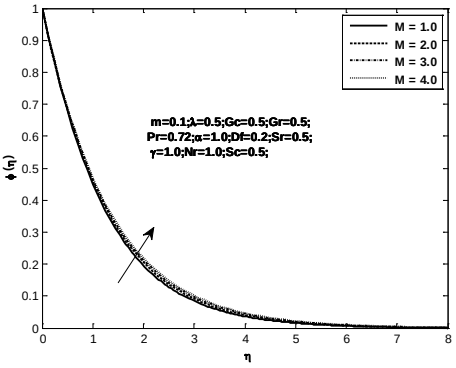

Fig. 5. Variation of $\varphi(\eta)$ with η for different values of M

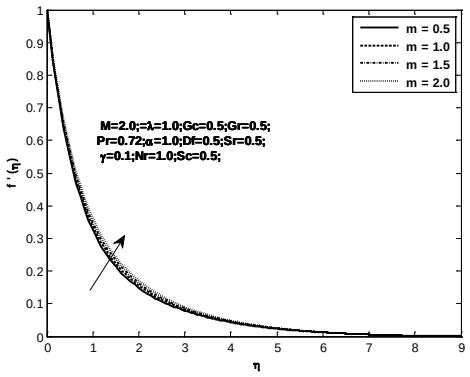

Fig. 6. Variation of f '(η) with η for different values of m

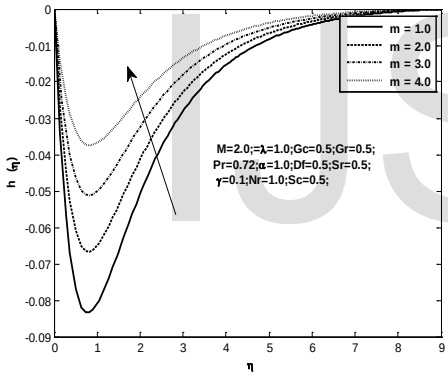

Fig. 7. Variation of h(η) with η for different values of m

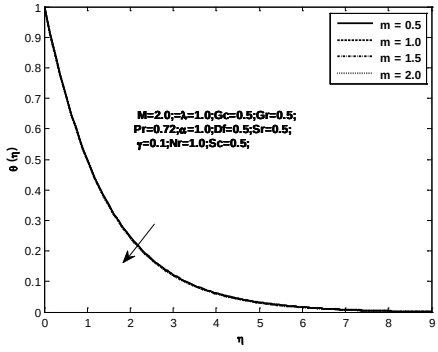

Fig. 8. Variation of θ(η) with η for different values of m

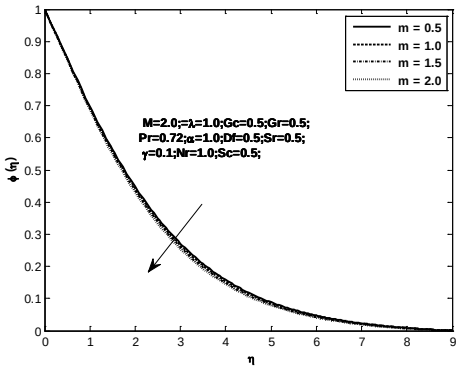

Fig. 9. Variation of $\varphi(\eta)$ with η for different values of m

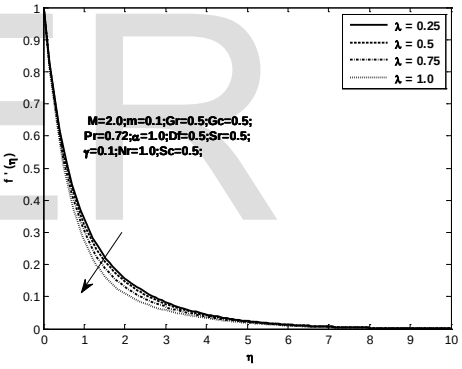

Fig. 10. Variation of f '(η) with η for different values of λ

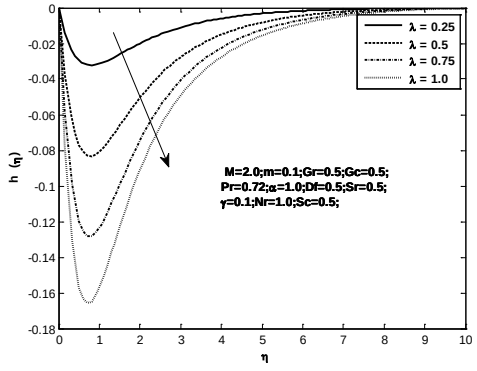

Fig. 11. Variation of h(η) with η for different values of λ

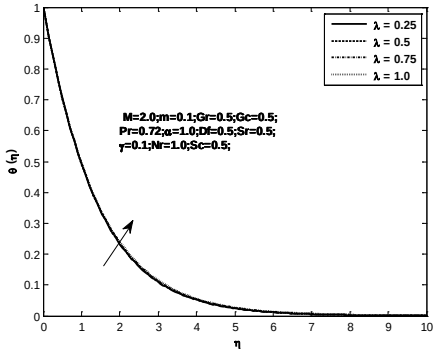

Fig. 12. Variation of θ(η) with η for different values of λ

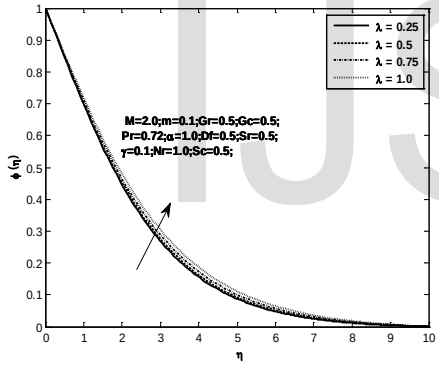

Fig. 13. Variation of φ(η) with η for different values of λ

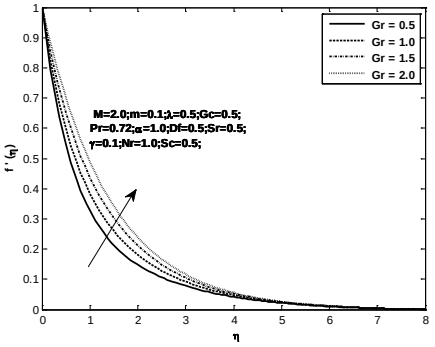

Fig. 14. Variation of f '(η) with η for different values of Gr

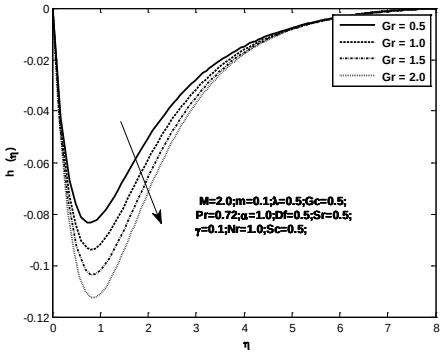

Fig. 15. Variation of h(η) with η for different values of Gr

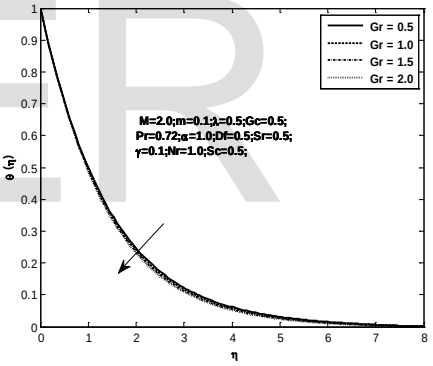

Fig. 16. Variation of θ(η) with η for different values of Gr

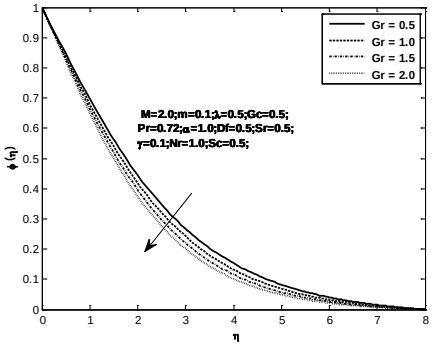

Fig. 17. Variation of $\varphi(\eta)$ with η for different values of Gr

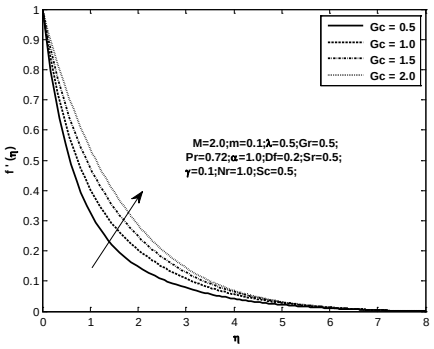

Fig. 18. Variation of f '(η) with η for different values of Gc

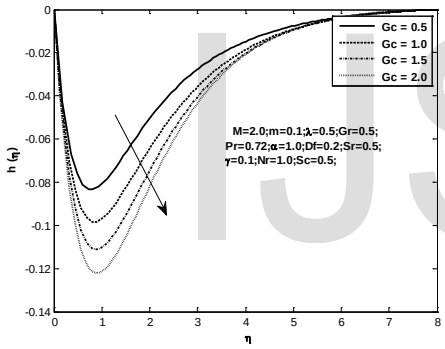

Fig. 19. Variation of h(η) with η for different values of Gc

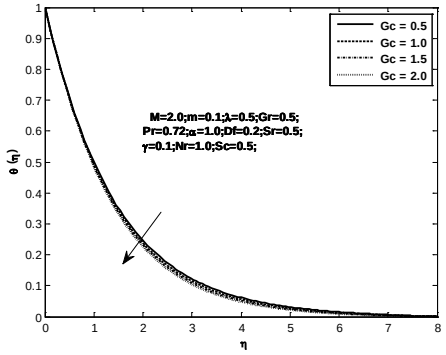

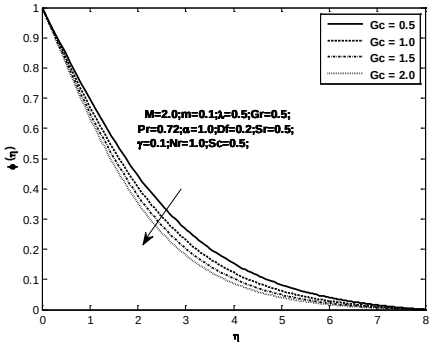

Fig. 21. Variation of $\varphi(\eta)$ with η for different values of Gc

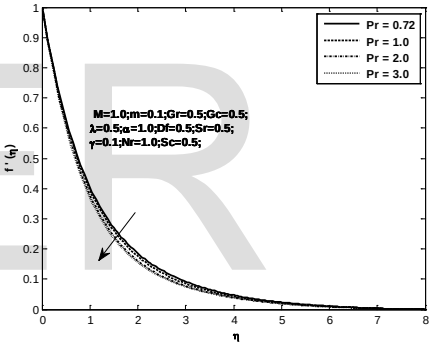

Fig. 22. Variation of f '(η) with η for different values of Pr

Fig.

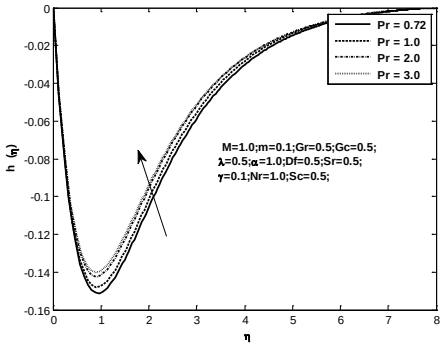

Fig. 23. Variation of h(η) with η for different values of Pr

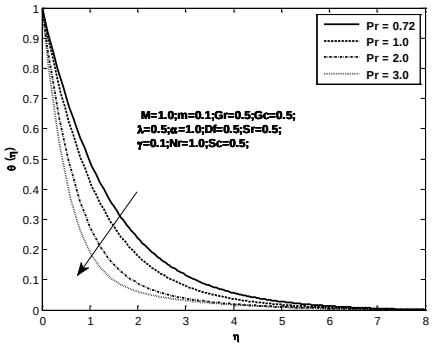

Fig. 24. Variation of θ(η) with η for different values of Pr

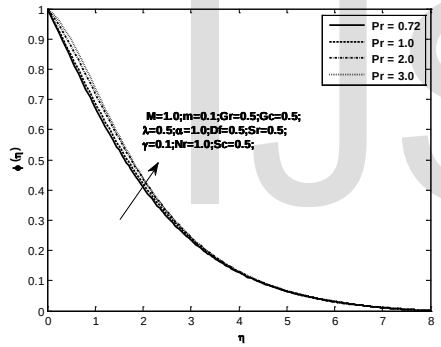

Fig. 25. Variation of $\varphi(\eta)$ with η for different values of Pr

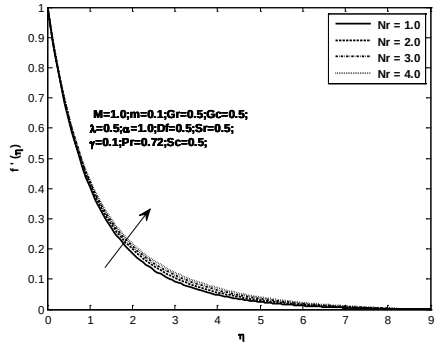

Fig. 26. Variation of f '(η) with η for different values of Nr

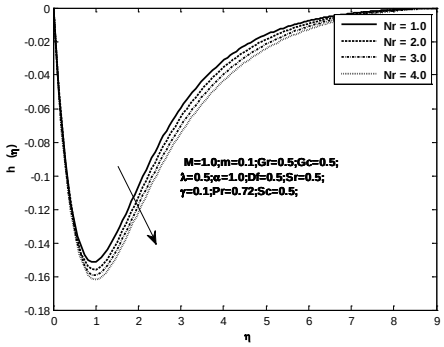

Fig. 27. Variation of h(η) with η for different values of Nr

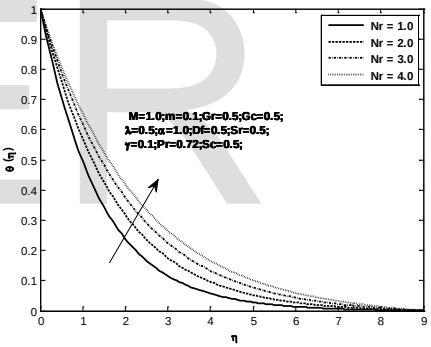

Fig. 28. Variation of θ(η) with η for different values of Nr

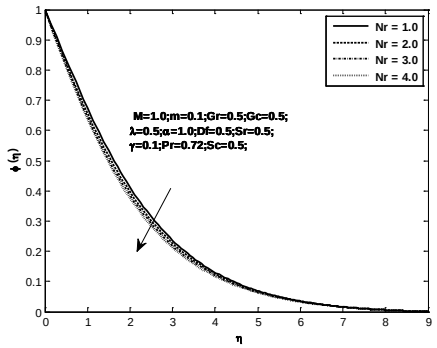

Fig. 29. Variation of $\varphi(\eta)$ with η for different values of Nr

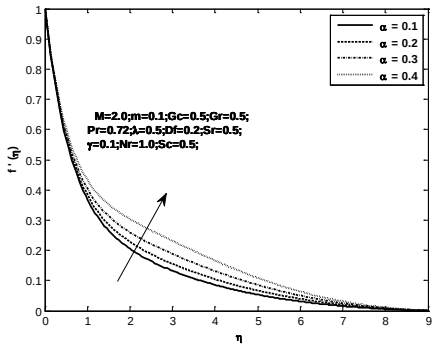

Fig. 30. Variation of f '(η) with η for different values of $\alpha > 0$

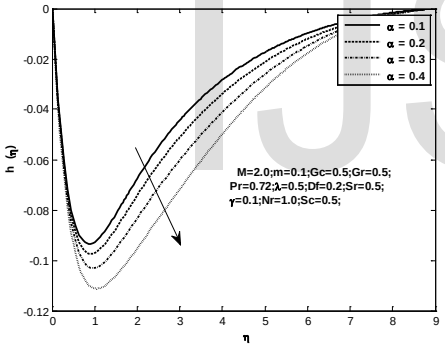

Fig. 31. Variation of h(η) with η for different values of $\alpha > 0$

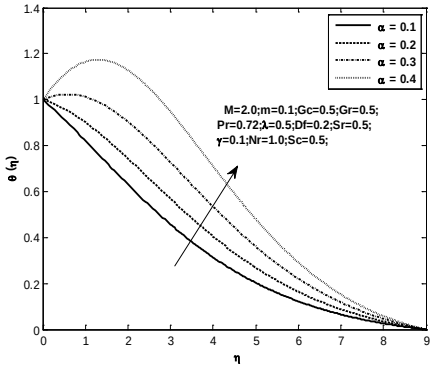

Fig. 3

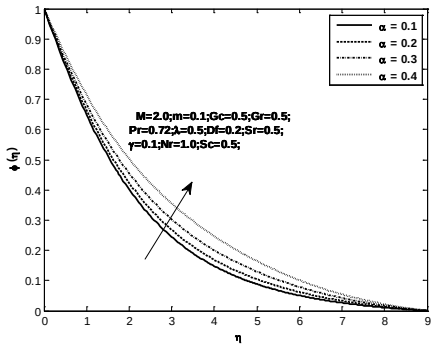

Fig. 33. Variation of $\varphi(\eta)$ with η for different values of $\alpha > 0$

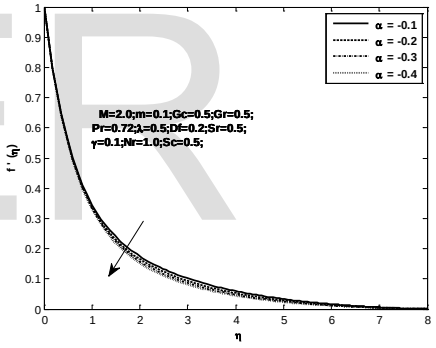

Fig. 34. Variation of f '(η) with η for different values of $\alpha < 0$

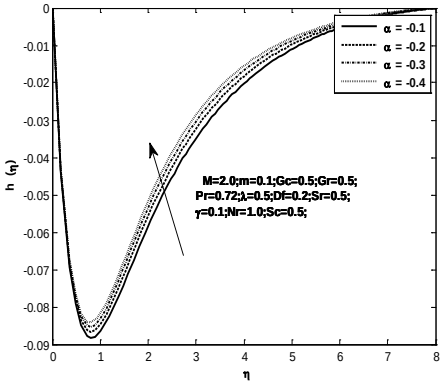

Fig. 35. Variation of h(η) with η for different values of $\alpha < 0$

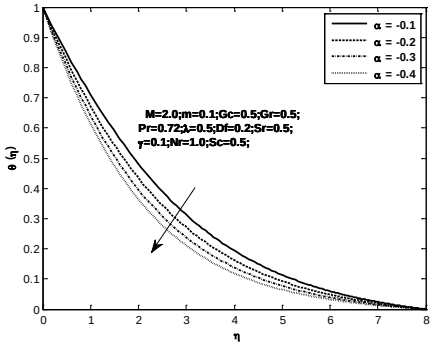

Fig. 36. Variation of θ(η) with η for different values of $\alpha < 0$

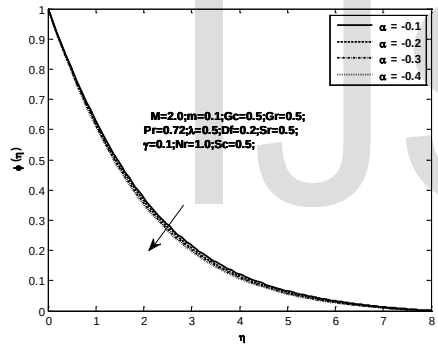

Fig. 37. Variation of $\varphi(\eta)$ with η for different values of $\alpha < 0$

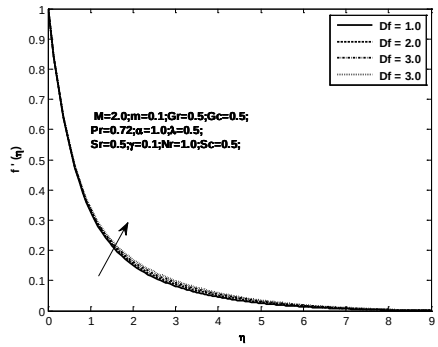

Fig. 38. Variation of f '(η) with η for different values of Df

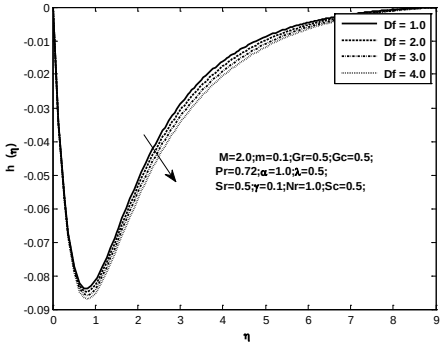

Fig. 39. Variation of h(η) with η for different values of Df

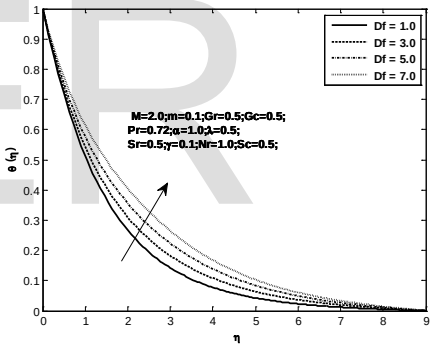

Fig. 40. Variation of θ(η) with η for different values of Df

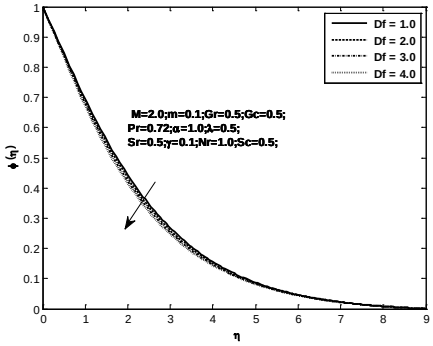

Fig. 41. Variation of $\varphi(\eta)$ with η for different values of Df

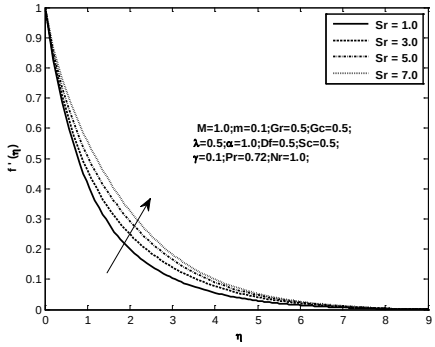

Fig. 42. Variation of f '(η) with η for different values of Sr

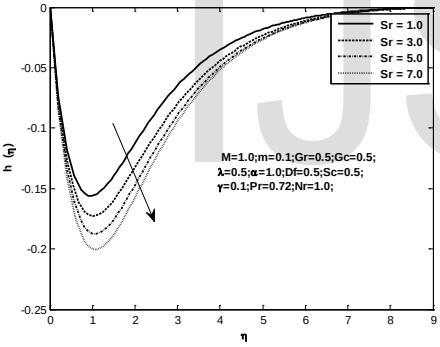

Fig. 43. Variation of h(η) with η for different values of Sr

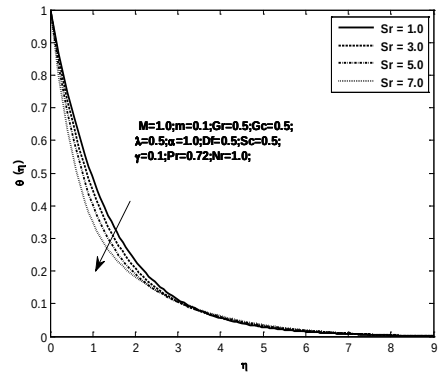

Fig. 44. Variation of θ(η) with η for different values of Sr

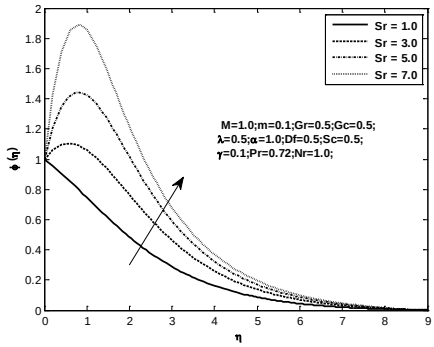

Fig. 45. Variation of $\varphi(\eta)$ with η for different values of Sr

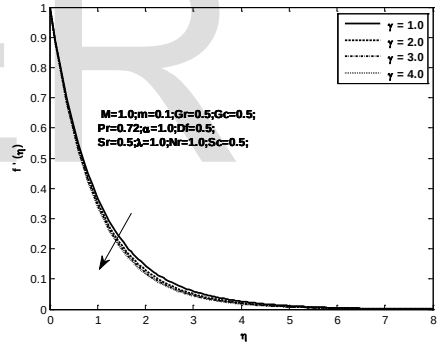

Fig. 46. Variation of f '(η) with η for different values of γ

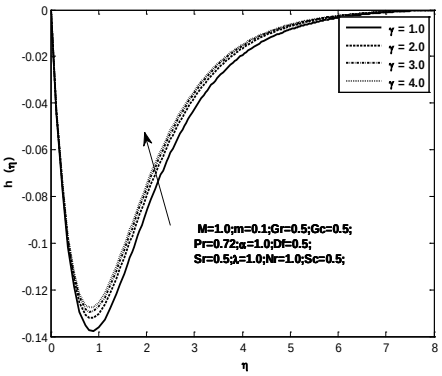

Fig. 47. Variation of h(η) with η for different values of γ

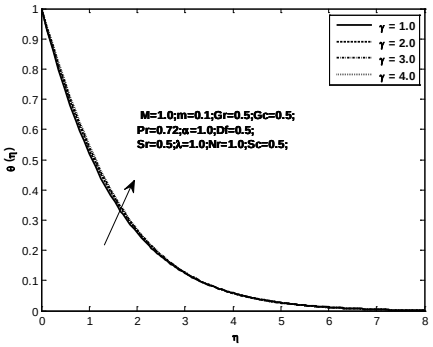

Fig. 48. Variation of θ(η) with η for different values of γ

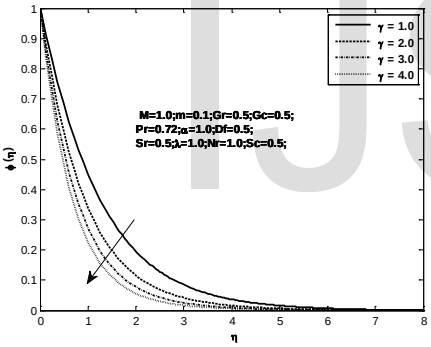

Fig. 49. Variation of $\varphi(\eta)$ with η for different values of γ

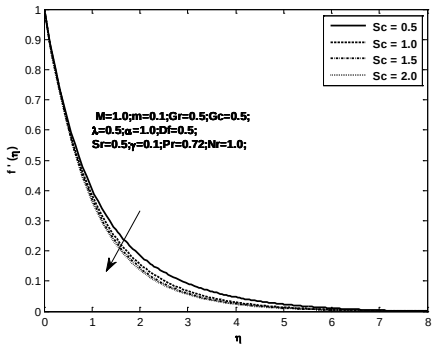

Fig. 50. Variation of f '(η) with η for different values of Sc

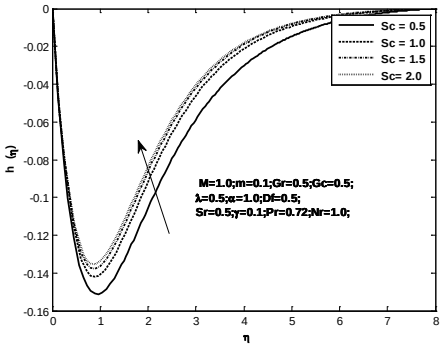

Fig. 51. Variation of h(η) with η for different values of Sc

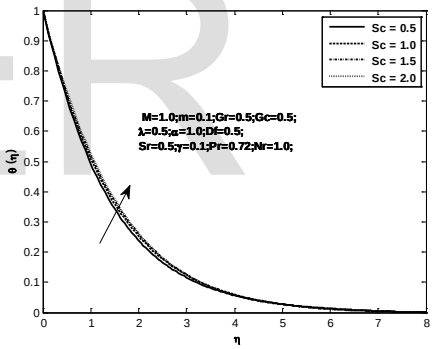

Fig. 52. Variation of θ(η) with η for different values of Sc

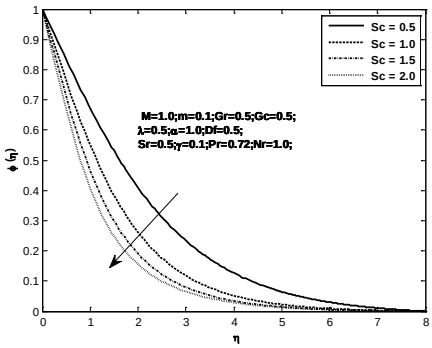

Fig. 53. Variation of $\varphi(\eta)$ with η for different

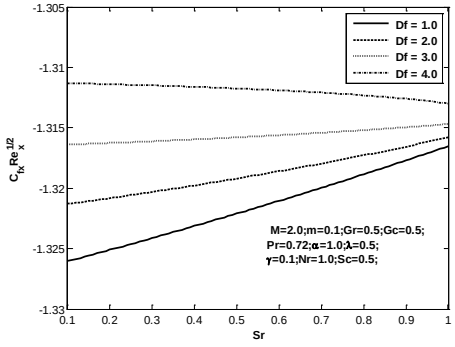

Fig. 54. Variation of Dufour number on the skin-friction coefficient.

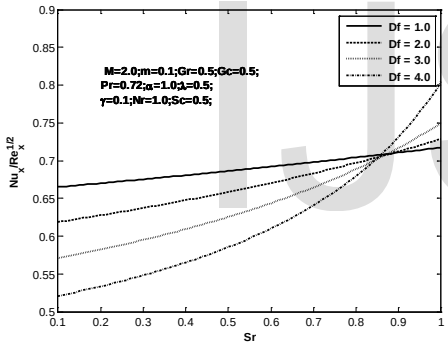

Fig.55 . Variation of Dufour number on the Nusselt number.

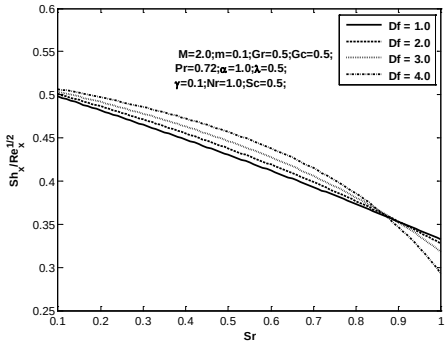

Fig. 56. Variation of Dufour number on the Sherwood number.

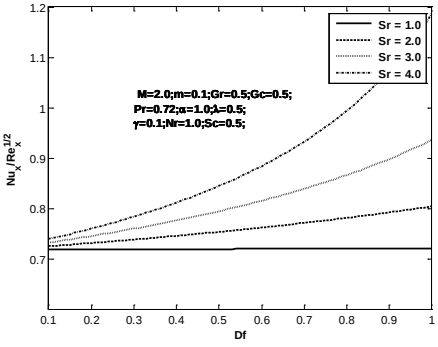

Fig. 57. Variation of Soret number on the Nusselt number.

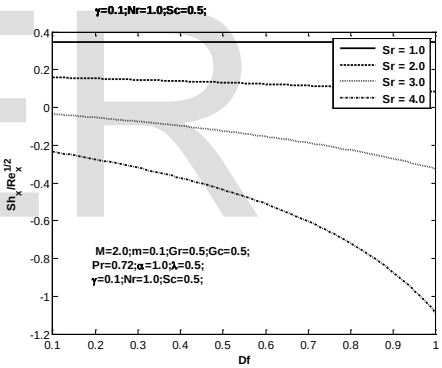

Fig. 58. Variation of Soret number on the Sherwood number.

TABLE 1

Values of $(Re_x)^{\frac{1}{2}}C_{fx}$ and $(Re_x)^{\frac{1}{2}}C_{fy}$ for different values of λ when M=0, m=0

λ	$(Re_x)^{\frac{1}{2}}C_{fx}$			$(Re_x)^{\frac{1}{2}}C_{fy}$		
	Wang[4]	Nazer et al.[7]	Present results	Wang[4]	Nazer et al.[7]	Present results
0.0	-1.0000	-1.0000	-1.0000	0.0000	0.0000	0.0000
0.2	-	-	-1.0331	-	-	-0.2385
0.4	-	-	-1.1009	-	-	-0.4310
0.5	-1.1384	-1.1384	-1.1384	-0.5128	-0.5128	-0.5128
0.6	-	-	-1.1764	-	-	-0.5874
0.8	-	-	-1.2518	-	-	-0.7204
1.0	-1.3250	-1.3250	-1.3250	-0.8371	-0.8371	-0.8371
1.2	-	-	-1.3956	-	-	-0.9420
1.4	-	-	-1.4634	-	-	-1.0379
1.6	-	-	-1.5287	-	-	-1.1265
1.8	-	-	-1.5916	-	-	-1.2093
2.0	-1.6523	-1.6523	-1.6523	-1.2873	-1.2873	-1.2873
3.0	-	-	-1.9289	-	-	-1.6248
4.0	-	-	-2.1716	-	-	-1.9054
5.0	-	-	-2.3901	-	-	-2.1506

TABLE 2

Skin friction coefficient, Nusselt number and Sherwood number for various values of pertinent parameters

M	m	λ	Gr	Gc	Pr	α	Nr	Df	γ	Sc	Sr	$f''(0)$	$h'(0)$	$-\theta'(0)$	$-\phi'(0)$
1.0												-0.997301	-0.417709	0.677074	0.747043
2.0	0.1	0.5	0.5	0.5	0.72	1.0	1.0	0.5	1.0	0.5	0.5	-1.331181	-0.289510	0.675915	0.737342
3.0												-1.623368	-0.211827	0.598708	0.729626
4.0												-1.881904	-0.158434	0.593803	0.723555
	0.1											-1.293842	-0.299019	0.668134	0.300716
2.0	0.2	0.5	0.5	0.5	0.72	1.0	1.0	0.5	0.1	0.5	0.5	-1.264095	-0.233934	0.668953	0.304422
	0.3											-1.226317	-0.175304	0.669890	0.308511
	0.4											-1.182462	-0.124780	0.670924	0.312902
		0.25										-1.272301	-0.113976	0.677705	0.302239
2.0	0.1	0.5	0.5	0.5	0.72	1.0	1.0	0.5	0.1	0.5	0.5	-1.294709	-0.298743	0.676772	0.297690
		0.75										-1.334451	-0.473793	0.673904	0.289772
		1.0										-1.387119	-0.635715	0.671332	0.279641
			0.5									-1.294174	-0.298878	0.668100	0.302573
2.0	0.1	0.5	1.0	0.5	0.72	1.0	1.0	0.5	0.1	0.5	0.5	-1.095505	-0.318297	0.672720	0.321370
			1.5									-0.899867	-0.328178	0.677180	0.338719
			2.0									-0.707045	-0.353797	0.681498	0.354786
				0.5								-1.294174	-0.298878	0.668100	0.302573
2.0	0.1	0.5	0.5	1.0	0.72	1.0	1.0	0.5	0.1	0.5	0.5	-1.066381	-0.324708	0.674209	0.329187
				1.5								-0.847577	-0.347289	0.679786	0.351221
				2.0								-0.635836	-0.367500	0.684959	0.351221
					0.72							-0.954806	-0.435159	0.674885	0.328337
1.0	0.1	0.5	0.5	0.5	1.0	1.0	1.0	0.5	0.1	0.5	0.5	-0.965995	-0.430975	0.808074	0.295609
					2.0							-0.991854	-0.423224	1.201012	0.200158
					3.0							-1.008084	-0.419527	1.541062	0.117818
						0.1						-1.245976	-0.312285	0.161225	0.391098
2.0	0.1	0.5	0.5	0.5	0.72	0.2	1.0	0.5	0.1	0.5	0.5	-1.229447	-0.317183	0.058320	0.372114
						0.3						-1.206717	-0.323912	-0.078160	0.346611
						0.4						-1.175300	-0.333032	-0.262311	0.310925
						-0.1						-1.268869	-0.305551	0.311270	0.419434
2.0	0.1	0.5	0.5	0.5	0.72	-0.2	1.0	0.5	0.1	0.5	0.5	-1.276645	-0.303394	0.366740	0.430302
						-0.3						-1.283271	-0.301593	0.415834	0.440089
						-0.4						-1.289038	-0.300059	0.460113	0.449063
							1.0					-0.954519	-0.435459	0.674909	0.326954
1.0	0.1	0.5	0.5	0.5	0.72	1.0	2.0	0.5	0.1	0.5	0.5	-0.941831	-0.440925	0.542679	0.359801
							3.0					-0.933670	-0.444870	0.466031	0.379117
							4.0					-0.927850	-0.447896	0.414726	0.392197
									1.0			-0.997301	-0.417709	0.612983	0.747043
1.0	0.1	0.5	0.5	0.5	0.72	1.0	1.0	0.5	2.0	0.5	0.5	-1.019139	-0.410332	0.567090	1.038479
									3.0			-1.032947	-0.406272	0.530297	1.265479
									4.0			-1.042952	-0.403616	0.498601	1.457792
										0.5		-0.954806	-0.435159	0.674885	0.328337
1.0	0.1	0.5	0.5	0.5	0.72	1.0	1.0	0.5	0.1	1.0	0.5	-0.977662	-0.423902	0.657246	0.467923
										1.5		-0.992316	-0.418211	0.641831	0.578491
										2.0		-1.002858	-0.414797	0.627710	0.674401

4 Conclusions:

The problem of mixed convection flow due to a stretching sheet in a rotating fluid in the presence of Soret, Dufour and thermal radiation with Hall currents is analysed. The partial differential equations describing the problem are transformed into the ordinary differential equations employing similarity transformations. The resulting equations are numerically solved by Runge – Kutta fourth order method along with shooting technique. From the analysis the salient features are presented below

(i) Higher the strength of the magnetic field lower the primary velocity distribution in the momentum boundary layer.

(ii) The effect of Hall parameter on all variables has an opposite trend to that of M.

(iii) The rotation parameter reduces both the velocities while it increases the temperature.

(iv) The Dufour and thermal radiation parameter and heat source parameter strongly enhance the temperature while the Pr, Sr and heat sink reduce the temperature.

(v) The Soret effect is increase the primary velocity and concentration with an overshoot of species concentration for higher values of Sr in the solutal boundary layer.

(vi) The Schmidt number and chemical reaction parameter significantly reduce the species concentration in the solutal boundary layer.

(vii) The skin friction coefficient in the x – direction decreases with M, γ while it increases with Du, Sr, Nr.

(viii) The Nusselt number decreases with Nr, Df, $\alpha > 0$, $\gamma > 0$ while Sr, Pr increases.

(ix) The Sherwood number increases with Df, γ and Sc while it decreases with Sr.

5 References:

1. Sakiadis B.C. "Boundary-layer behavior on continuous solid surfaces: II. The boundary layer on a continuous flat surface". AIChE J;7:221 – 227, 1961
2. Crane, L. J., "Flow past a stretching plate," Z. Angew Math Phys 21, 645-7, 1970
3. L. J. Crane, Z. Angew Math. Mech 82, 984, 1982.
4. C. Y. Wang, "Stretching a surface in a rotating fluid", ZAMP 39 177 – 185, 1988
5. H.S. Takhar, A.J. Chamkha, G. Nath, "MHD flow over a moving plate in a rotating fluid with magnetic field, Hall currents and free stream velocity," *International Journal of Engineering Science* 40 1511 – 1527, 2002
6. Nisat Nowroz Anika, Md. Mainual Hoque, Nazmul Islam, "Hall Current Effects on Magnetohydrodynamics Fluid over an Infinite Rotating Vertical Porous Plate Embedded in Unsteady Laminar Flow," *Annals of Pure and Applied Mathematics*, Vol. 3, No.2,, 189 – 200, 2013
7. Nazar, R., Amin, N., and Pop, I. "Unsteady boundaru layer flow due to a stretching surface in a rotating fluid," *Mechanics Research Communications*, 31 (1), 121 – 128, 2004